International Symposium on
HYDROACOUSTICS AND ULTRASONICS
EAA Symposium (formerly 13th FASE Symposium)
Gdańsk-Jurata, 12-16 May 1997

SPATIAL DISTRIBUTIONS OF ACOUSTIC FIELD SCATTERED AT THE SEA BOTTOM - NUMERICAL MODEL

Jarosław Tęgowski
Institute of Oceanology Polish Academy of Sciences,
Powstanców Warszawy 55, 81-712 Sopot, Poland

ABSTRACT

The results of the numerical simulation of acoustic wave scattering from rough and attenuating sea bottom are presented. Scattering is studied using ray theory with the main geometry of model taken from Novarini and Caruthers [4]. The distribution of rough surface heights together with bottom acoustical parameters determine the scattered acoustical field properties. Different bottom types with various acoustical parameters have been used in numerical calculations in order to examine the influence of phase shift of reflected signal on scattered acoustical field. Simulation technique was made for surfaces with normal distribution of heights and standard deviation of the surface elevation, 0.01 m. Spatial distribution of the scattered field parameters was determined. Results of calculations for frequencies between 5 and 100 kHz and various bottom parameters are compared.

INTRODUCTION

The roughness of marine bottom floor and sound attenuation at the top layer of sediments influence acoustic field reflected and scattered at the sea-bed. Despite a large volume of theoretical and experimental works concerning scattering problem there has been no sufficient description of this phenomena. The dependence between statistical parameters of corrugated surface and parameters of scattered acoustical field have been shown. However, such important as a phase shift of signal reflected from the attenuating bottom surface has not been taken into account. The subject of this work is an examination of its on scattered field parameters.

Presented model is a specific implementation of the Caruthers and Novarini [4] numerical simulation technique of acoustic scattering at randomly rough sea surface. Basic geometry and way of surface construction are based on a facet model. The novelty is the application of attenuating and scattering surface with statistical and acoustical parameters adequate to the top layer of the bottom sediments.

An application of image method is based on the simulations of reflections from elementary facets imitating rough surface with the Gaussian height distribution. Computations of scattered field parameters have been made for a net of hydrophones placed in the perpendicular direction to specular reflection. Frequency dependences of total and coherent intensity, degree of coherence, amplitude fluctuations and spatial correlations in horizontal and vertical directions have been investigated and compared for sediments with acoustical parameters of Baltic sands, clays and silts.

DESCRIPTION OF THE MODEL

The method of scattering simulation was based on the ray acoustic approximation. The position of the source, hydrophones and bottom surface were simulated like in a natural experiment (see Figure 1.a.).

The basic assumptions of the model were:

- neglect of the scattering from subbottom layers,
- multiple scattering effects not included (scattered energy was not rescattered),
- shadowing and refractioning effects not taken into account,
- constant sound speed c_1 in the sea water.

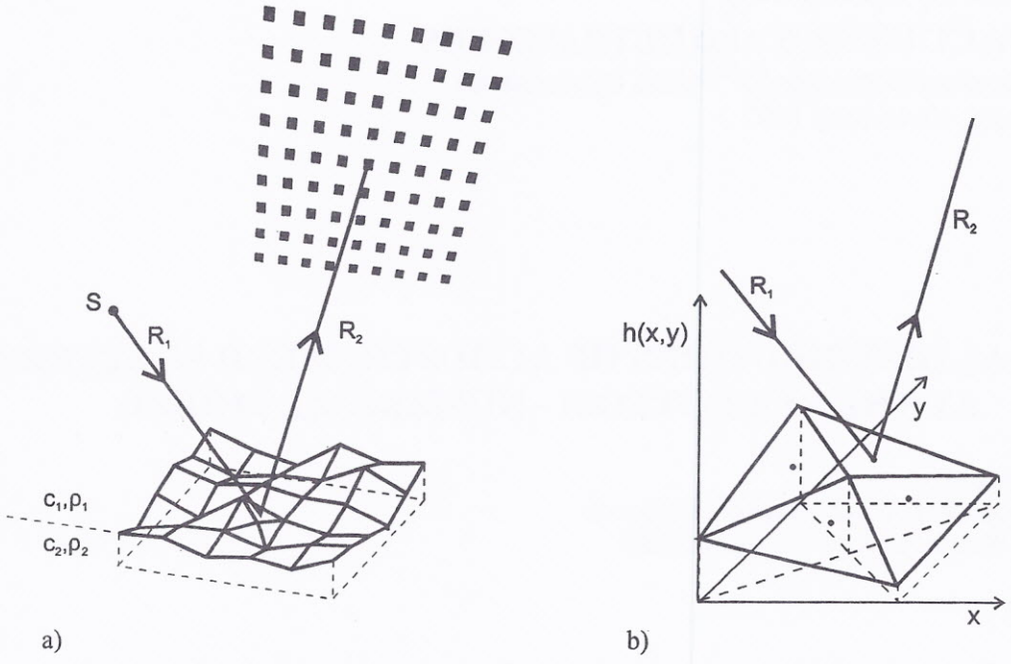

Fig.1.a) Model geometry. b) Coordinate system for reflection at the bottom facet.

Figure 1.a. illustrates the main geometry of the model. Omnidirectional source of acoustical signals is located at distance R_1=25 m from the centre of the ensonified area. Signals emitted by transducer are reflected from each bottom facet which is considered a unidirectional reflector. The direction of reflection is determined as [4]:

$$\bar{n} = s\left(\bar{i} + \bar{r}\right), \qquad (1)$$

where $\bar{i}$, $\bar{r}$ and $\bar{n}$ are unit vectors of incident, reflected and facet normal ray, respectively, and s is a proportional factor.

Rough surface scatters incident wave into different directions due to inclination angles of facets. The part of this area is shown in detail in Figure. 1.b. Construction of irregular surface follows. At the first step a set of 11x11 random, uncorelated numbers having zero mean and normal distribution is generated. That numbers create a square net of surface elevation hights h(x,y) separated by $\Delta x = \Delta y = 0.4\,\mathrm{m}$. Each square element is divided to four triangles with elevation of centre being the arithmetical average of corners heights. Gravity centre of each triangle is the place of specular reflection of the incident wave. This procedure smoothes irregular surface and reduces the edge effect. Sizes of facets and statistical parameters of the surface determine the frequency of incident waves in order to obey the Kirchhoff approximation, which requires every part of a scattering surface to be locally planar related to direction of the incident ray. On the other hand, surface deviations must be much smaller than the wavelength.

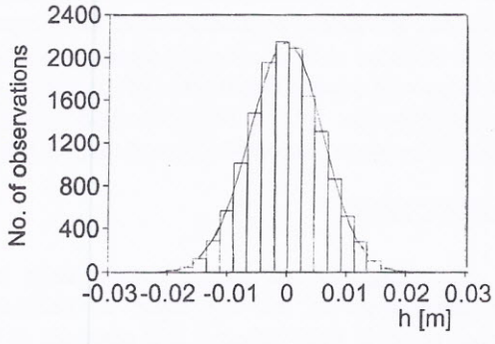

Fig.2. Histogram of the surface heights, (δH=0.01m, correlation length 0.7 m).

That implies the condition on the wavelength of incident wave:

$$\delta h \langle \lambda \langle \Delta x, \Delta y\,, \qquad (2)$$

where $\delta h = 0.01\mathrm{m}$ is the standard deviation of the elevation and $\Delta x, \Delta y$ are the horizontal sizes of scattering facets. In a consequence, the frequency was chosen at the interval from 5 to 100 kHz. For used angles of incidence (θ_1 = 40°, 60° and 75°) a Rayleigh parameter ($P = 2k\delta h \cos\theta_1$, where k - wave number) varies from nearly 0 to 6, i.e., from acoustically smooth to rough surface. At $P << 1$ the surface scatters energy in the specular direction and $P >> 1$ causes that sound is scattered in a relatively wide

angular interval. A source-bottom distance influences the statistical parameters of scattered field. Ensofonied surface comprises the first several Fresnel zones with radii dependent on incident wave frequency. Therefore diffraction effects will be visible in spatial and fre-quency distributions of the acoustic pressures.

Spatial distributions of acoustic pressure are calculated for a 9x9 flat net of omnidirectional hydrophones (Fig 1.a). Receiver plane is perpendicular to the centre facet of the flat bottom. Its distance is R_2=25. The area of the hydrophones net is big enough to register the whole energy scattered from the flat bottom in the case of normal incidence. The distance between hydrophones is $\Delta X=\Delta Y$=1m.

Apart from statistical parameters of the rough surface, also the physical parameters of sediments influence the scattered acoustical field. Therefore a set of Baltic sediment parameters taken from [5] and our own works is used in the model. There are collected in Table 1.

Table 1. Parameters of sediments used in model (density ρ, sound velocity c and attenuation coefficient α_e).

parameter	sand	clay	silt
ρ [g/cm^3]	2.01	1.41	1.22
c [m/s]	1750	1500	1400
α_e [dB/m/kHz]	0.67	0.075	0.24

Those parameters are applied for calculating of reflection coefficient $V(\theta_1,\alpha_e,\rho,c)$ and phase shift $\varphi(\theta_1,\alpha_e,\rho,c)$ of reflected waves from attenuating bottom [1, 5].

PARAMETERS OF SCATTERED FIELD

In order to calculate statistical parameters of scattered field, a numerical simulation was performed for L=30 independent surfaces with the same statistical and physical parameters. The results were averaged.

Pressure of wave scattered from bottom elements labelled (n,m) was calculated for each hydrophone (i,j):

$$p_{i,j,l}(n,m)=\sum_{n}^{N1}\sum_{m}^{N2}p_{n,m}\,, \qquad (3)$$

where

$$p_{n,m}=V(\theta_1,\alpha_e,\rho,c)\cdot\frac{1}{R}e^{i\left[kR-\varphi(\theta_1,\alpha_e,\rho,c)\right]}\,, \qquad (4)$$

$p_{n,m}$ - pressure of wave arise from reflection at facet (m,n),

l - counts the number of rough surface,

N1 - number of square scattering elements of the bottom surface,

N2=4 - number of triangles in n-th scattering square,

$R=R_1+R_2$ - the distance from the source to the bottom facet and from the facet to the hydrophone.

The average pressure registered at hydrophone (i,j) is calculated from:

$$\langle p\rangle\equiv\langle p_{i,j}\rangle=\frac{1}{L}\sum_{l=1}^{L}p_{i,j,l}(n,m)\,. \qquad (5)$$

From there appears the formulas descripting parameters of scattered field [3,4]:

mean intensity

$$I_m=\frac{\langle p\cdot p^*\rangle}{\rho_2 c_2}=\frac{1}{\rho_2 c_2}\frac{1}{L}\sum_{l=1}^{L}p_l\cdot p_l^*\,, \qquad 6)$$

coherent part of intensity

$$I_{coh}=\frac{\langle p\rangle\cdot\langle p^*\rangle}{\rho_2 c_2}\,, \qquad (7)$$

incoherent part of intensity

$$I_{incoh}=\frac{1}{\rho\cdot c}\langle p\cdot p^*\rangle-\langle p\rangle\cdot\langle p^*\rangle=I_m-I_{coh}\,, \qquad (8)$$

degree of coherence

$$Coh=\left(\frac{\langle p\rangle\langle p^*\rangle}{\langle p\cdot p^*\rangle}\right)^{\frac{1}{2}}=\sqrt{\frac{I_{coh}}{I_m}}\,, \qquad (9)$$

amplitude fluctuations

$$A_f=\sqrt{\frac{I_{incoh}}{I_{coh}}}\,, \qquad (10)$$

spatial correlation function

$$\Gamma=\langle p_a p_b^*\rangle=\frac{1}{L}\sum_{i=1}^{L}p_{a,i}p_{b,i}^* \qquad (11)$$

total pressure

$$P_{tot}=\sum_{i=1}^{9}\sum_{j=1}^{9}\langle p_{i,j}\rangle\,. \qquad (12)$$

RESULTS

The main goal of this work was to examine the influence of phase shift of reflected signal on scattered acoustical field. *In situ* or laboratory measurements of these dependences are practically unrealisable. Presented results are shown a relationships between scattered field parameters and factors influencing them. Numerical simulations were performed for wide frequency diapason of incident wave, three sets of sediments parameters, three incident angles closed to critical reflection angle and fixed parameters of rough surface. The results of calculation were not normalised and there are presented in arbitrary units. Figures 3-6 show a coherent part of intensity and a degree of coherence for various cases. Thick lines in represent calculations with taking into account the phase shift in formula 4 . Thin lines represent the case without taking it into account.

Figure 2 shows the spatial distributions of the acoustic wave pressure as viewed of the backside of the hydrophones net. The parameters of simulation were: angle of incidence 60°, frequency 10 kHz and elastic parameters for silt. For both figures the maximum values of pressure are placed at the central part of the net. The reason for this is a scattering of main part of incident energy in specular direction.

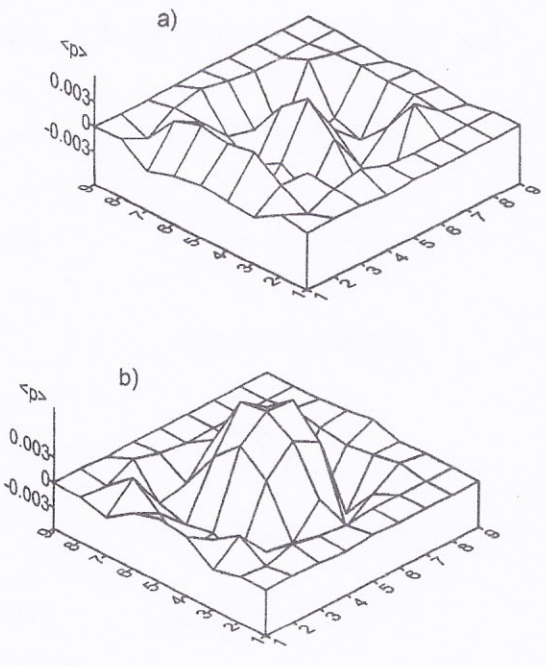

Fig.2. Spatial distributions of the acoustic wave pressure for angle of incidence 60°, frequency 10 kHz and silt. Figure 2.a) is regarded to phase shift, 2.b) without taking it into account.

Figures 2.a) and 2.b) reveal the differences between pressure calculations for examined cases. Introduction of phase shift in reflected signals changes pressure spatial distributions. For set of bottom types used in model this effect is the greatest for silt because the acoustical parameters of this sediment cause the biggest phase shift of reflected wave for analysed angle of incidence.

Figure 3 gives coherent part of the scattered signal intensity (formula 7) calculated at the centre hydrophone (5,5) as a function of a Rayleigh parameter. Simulations were performed for angle of incidence 60°, sand, clay and for silt.

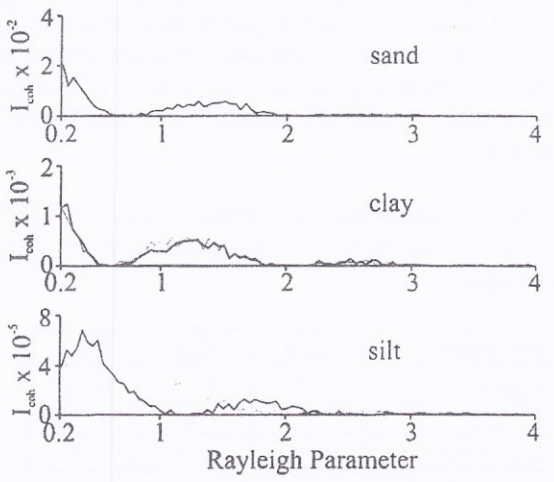

Fig.3. Coherent intensity of scattered calculated at central hydrophone (5,5) as a function of a Rayleigh parameter. Angle of incidence 60°, sand, clay and silt successively.

As we can expect, the coherent intensity decrease with the increasing Rayleigh parameter. The coherent intensity fluctuations are the result of the scattering at surfaces with several Fresnel zones with radii dependent on incident wave frequency. Therefore diffraction effects are visible in these results.

The diferences in values of coherent intensity in cases of taking into account the phase shift φ and without it (thick and thin lines) are the direct result of different attenuating properties of sediments.

The next two figures show the dependence of the degree of coherence (formula 9) upon the incident wave frequency and roughness parameter for sand (Fig. 4) and silt (Fig. 5). This simulation was performed for the central line of hydrophones (5,i) placed paralelly to the plane of the specular reflection. The angle of incidence was choosen 60°. The reason for that is the rapid increase of reflection coefficient and phase shift values for this angle. The degree of coherence is greatest for central set of hydrophones and decreases in direction of upper and lower one.

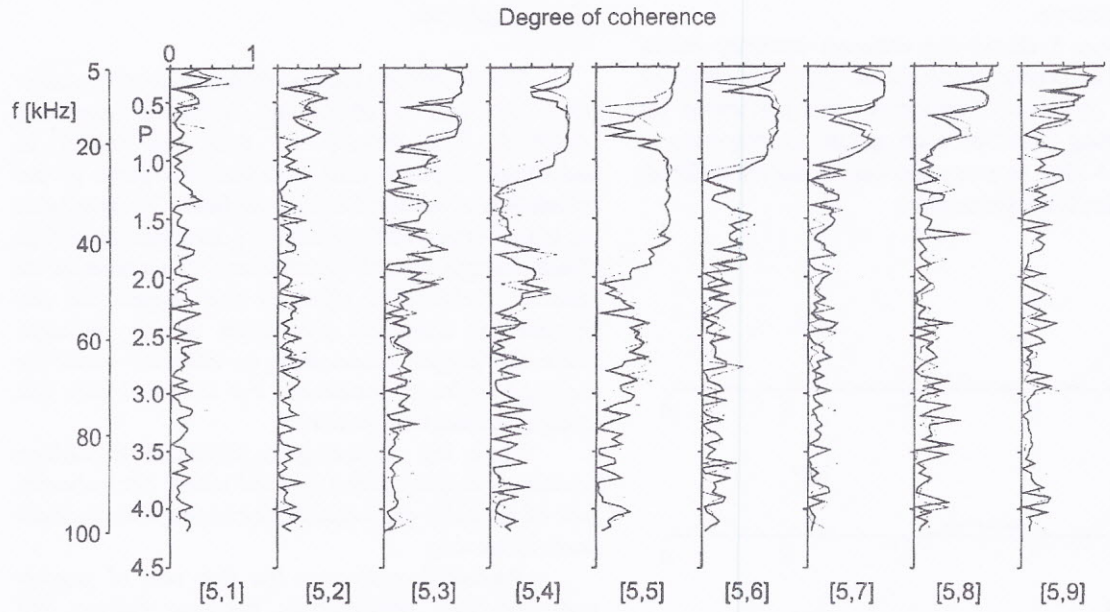

Fig.4. Dependence of the degre of coherence upon the incident wave freqency and Rayleigh parameter for sand. Simulation was performed for center array of hydrophones placed paralelly to incident wave plane and angle of incidence 60°. At the bottom of figure are marked a hydrophone numbers.

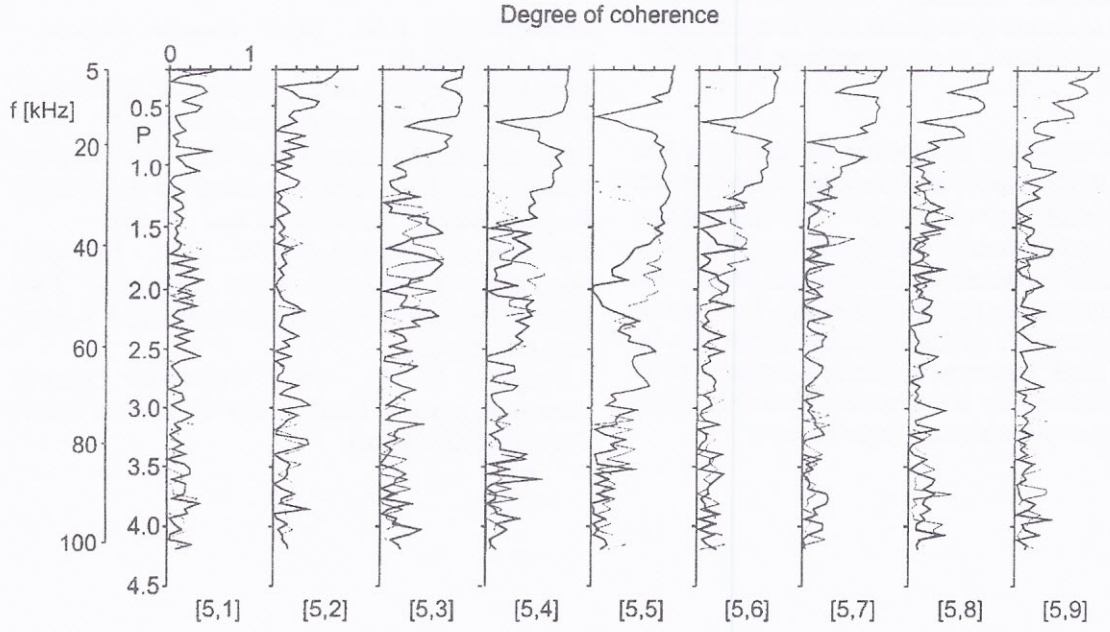

Fig.5. Dependence of the degre of coherence upon the incident wave freqency and Rayleigh parameter for silt. Simulation was performed for center array of hydrophones placed paralelly to incident wave plane and angle of incidence 60°. At the bottom of figure are marked a hydrophone numbers.

This is a result of considerable phase fluctuations in the net edges. Scattered field is coherent only in a narrow cone enclosing a specular direction. For small values of Rayleigh parameter, the value of coherence is the greatest and it falls with roughness parameter and frequency increasing. At the central hydrophone (5,5) the rapid fall of coherence appears after exceeding the value of roughness parameter 2. For other hydrophones a such behaviour of coherence starts earlier. There are certain differences in shapes of coherence for sand (Fig.4) and silt (Fig.5). The influence of phase shift on this parameter for first sediment is not big but appreciable. For silt however the phase shift in reflected signal changes shapes of a

coherence curve.

Figure 5 shows the coherent intensity calculated on the central hydrophone (5,5) for different angles of incidence. Simulations are performed for sand. Starting point of each graphs corresponds to frequency 5 kHz, so presented curves start at different values of Rayleigh parameter.

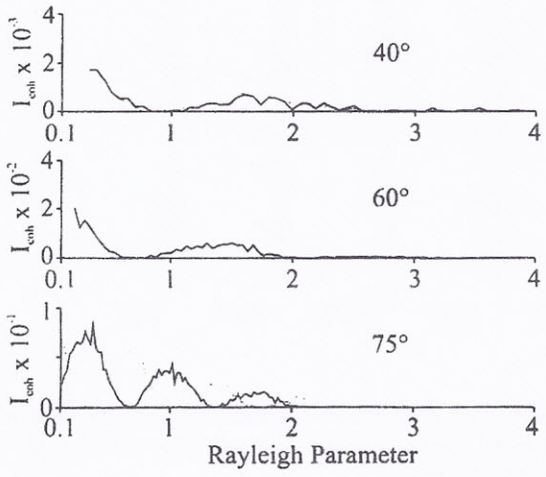

Fig.6. Coherent intensity of scattered signal calculated at central hydrophone (5,5) as a function of a Rayleigh parameter. Angle of incidence 40° 60° 75°, sand.

The behaviour of coherent intensity as a function of a Rayleigh parameter is similar to the previous figures. Intensity decreases with increasing roughness parameter and frequency of incident wave. The values of calculated parameter reach minimum at 40° and increase as the angle incidence increases. It reflect the angular dependence of the reflection coefficient. On the other hand, appearing of above mentioned effect could be induced by the acoustical flattening of the rough surface when incident angle increase.

CONCLUSIONS

The simulation method of acoustic wave scattering from rough and attenuating sea bottom have been presented. The novelty of presented model is including the phase shift of reflected signals to the calculation of scattered acoustical field. Compare with the older version of the model [4], introduction of this effect changes spatial distributions of parameters of scattered field. This effect is the highest for silt because the acoustical parameters of this sediment cause the biggest phase shift in reflected wave for analysed angles of incidence. For sand and clay this effect is substantially lower.

Since the scattering is simulated at surface containing a first several Fresnel zones, the coherent part of intensity periodically fluctuated with incident wave increasing.

Presented results are the first part of angular and frequency dependences between bottom and scattered field parameters. The more complete study will be presented.

REFERENCES

1.Brechowskich L.M., 1974, *Akustika Okieana* - Nauka, Moskov, 94.

2.Mackenzie K.V., 1960, *Reflection of Sound from Coastal Bottoms*, J. Acoust. Soc. Am. 51, 417.

3.Novarini J.C., Caruthers J.W., 1972, - *The Degree of Coherence of Acoustic Signals Scattered at Randomly Rough Surfaces*, J. Acoust. Soc. Am. 32, 221

4.Novarini J. C., Caruthers J. W., 1973, - *Numerical Modelling of Acoustic Wave Scattering from Randomly Rough Surfaces: A Facet Model*, J. Acoust. Soc. Am. 53, 876.

5..Svirydov N. L., 1980, *Fiziczeskije svojstva korennych porod i osadkov dna Baltijskovo moria*, Sovietskaja Geologia 3.